Electronic Supplementary Material (ESI) for Journal of Materials Chemistry A.

Asymmetric nonfullerene acceptors with isomeric trifluorobenzene-substitution for high-performance organic solar cells

Contents

1. Materials and Synthesis

Materials: All the other chemicals were purchased as reagent grade from J&K, Macklin, and Bidepharm, and used without further purification. All solvents for reactions were accessed through commercial channels and distilled immediately prior to use.

Compound 4: a mixture of compound **2** (100 mg, 0.3677 mmol), $Pd(dpppf)Cl_2$ (13.4 mg, 0.0184 mmol), $CsCO_3$ (596.5 mg, 1.8385 mmol), (4,5,6-Trifluorophenyl) boronic acid (644mg, 3.66mmol) in DMSO (20 ml) and H_2O (5 ml) was reacted 12 hours under Argon at 110 ℃. The reaction mixture was then cooled to room temperature and then extracted with dichlone. The organic layer was washed with brine and dried over $MgSO_4$. After filtration, the crude product was purified by flash column chromatography with petroleum ether and dichlone (4:1) as the eluents to afford the final product as light red solid. (75 mg, 62.9%).**^{1}H NMR** (400 MHz, $CDCl_3$) δ: 8.75 (s, 1H), 8.06-8.08 (d, 1H), 7.97-7.99 (d, 1H), 7.21-7.27 (m, 1H), 7.12-7.19 (m, 1H), 3.79 (s, 2H).

Compound 5: a mixture of compound **3** (100 mg, 0.3677 mmol), $Pd(dpppf)Cl_2$ (13.4 mg, 0.0184 mmol), $CsCO_3$ (596.5 mg, 1.8385 mmol), (4,5,6-Trifluorophenyl) boronic acid (644 mg, 3.66 mmol) in DMSO (12 ml) and H_2O (3 ml) was reacted 12 hours under Argon at 110 ℃. The reaction mixture was then cooled to room temperature and then extracted with dichlone. The organic layer was washed with brine and dried over MgSO4. After filtration, the crude product was purified by flash column chromatography with petroleum ether and dichlone (4:1) as the eluents to afford the final product as light red solid. (93 mg, 78%).**^{1}H NMR** (400 MHz, $CDCl_3$) δ: 8.72-8.75 (d, 1H), 8.1 (s, 1H), 8.02-8.05 (dt, 1H), 7.22-7.28 (m, 1H), 7.12-7.19 (m, 1H), 3.79 (s, 2H).

Compound BTP-β-Ar3F: a mixture of compound **6** (0.25 g, 0.185 mmol), compound **4** (0.066 g, 0.2035 mmol), $B_3F{\cdot}C_2H_5OC_2H_5$ (0.01 ml), Ac_2O (0.04 ml) in toluene (5 ml) was reacted 1 hour at 60℃. The reaction mixture was then cooled to room temperature and then centrifugal separation with methanol. The crude product was purified by flash column chromatography with petroleum ether and dichloromethane (1:1) as the eluents to afford the final product as red oily liquid. (0.286 g, 93.2%). **^{1}H NMR** (400 MHz, $CDCl_3$) δ: 9.20 (s, 1H), 9.16 (s, 1H), 8.78-8.80 (d, 1H), 8.55-8.59 (q, 1H), 8.08 (s, 1H), 7.89-7.91 (d, 1H), 7.68-7.72 (t, 1H), 7.26-7.31 (m, 1H), 7.13-7.19 (m, 1H), 4.72-4.82 (m, 4H), 3.22-3.27 (q, 4H), 2.10-2.19 (m, 2H), 1.84-1.93 (m, 4H), 1.48-1.61 (m, 9H), 0.85-1.38 (m, 61H), 0.61-0.72 (m, 12H). **^{13}C NMR**

(100MHz, $CDCl_3$) δ: 187.95, 186.06, 159.90, 158.65, 153.84, 153.27, 152.98, 147.34, 145.11, 145.05, 139.44, 137.84, 137.35, 136.64, 136.10, 135.60, 135.10, 134.50, 134.12, 133.77, 133.45, 133.21, 130.72, 130.26, 125.50, 123.84, 123.50, 120.77, 119.79, 115.28, 114.96, 114.86, 114.56, 113.66, 113.48, 113.03, 112.90, 68.56, 68.29, 55.79, 39.21, 31.91, 31.60, 31.21, 31.16, 30.46, 29.83, 29.66, 29.62, 29.52, 29.48, 29.34, 28.05, 27.90, 25.51, 25.34, 22.92, 22.88, 22.84, 22.68, 22.50, 14.11, 14.02, 13.99, 13.82, 13.78, 13.75.

Compound BTP-γ-Ar3F: a mixture of compound **6** (0.25 g, 0.185 mmol), compound **5** (0.066 g, 0.2035 mmol), $B_3F{\cdot}C_2H_5OC_2H_5$ (0.01 ml), Ac_2O (0.04 ml) in toluene (5 ml) was reacted 1 hour at 60℃. The reaction mixture was then cooled to room temperature and then centrifugal separation with methanol. The crude product was purified by flash column chromatography with petroleum ether and dichloromethane (1:1) as the eluents to afford the final product as blue solid. (0.28 g, 92%). **^{1}H NMR** (400 MHz, CDCl3) δ: 9.20 (s, 1H), 9.16 (s, 1H), 8.83 (s, 1H), 8.54-8.58 (q, 1H), 8.01-8.03 (d, 1H), 7.90-7.92 (d, 1H), 7.68-7.72 (t, 1H), 7.26-7.31 (m, 1H), 7.11-7.17 (m, 1H), 4.72-4.83 (m, 4H), 3.21-3.27 (q, 4H), 2.10-2.19 (m, 2H), 1.84-1.93 (m, 4H), 1.51-1.57 (m, 9H), 0.84-1.37 (m, 61H), 0.63-0.73 (m, 12H). **^{13}C NMR** (100MHz, $CDCl_3$) δ: 187.80, 186.05, 160.18, 158.66, 153.84, 153.29, 153.08, 152.98, 147.34, 145.12, 140.87, 140.46, 137.86, 137.64, 136.22, 136.10, 135.63, 135.15, 134.78, 134.45, 134.13, 133.79, 133.48, 133.22, 130.77, 130.25, 125.17, 124.88, 123.97, 123.73, 120.87, 119.79, 115.22, 115.00, 114.96, 114.81, 114.56, 113.68, 113.47, 113.09, 112.91, 112.47, 112.28, 68.56, 68.46, 55.80, 39.22, 31.92, 31.61, 31.58, 31.22, 31.19, 30.45, 29.83, 29.66, 29.62, 29.52, 29.48, 29.34, 28.08, 27.93, 25.48, 25.31, 22.88, 22.85, 22.68, 22.50, 14.11, 14.02, 13.83, 13.79, 13.77.

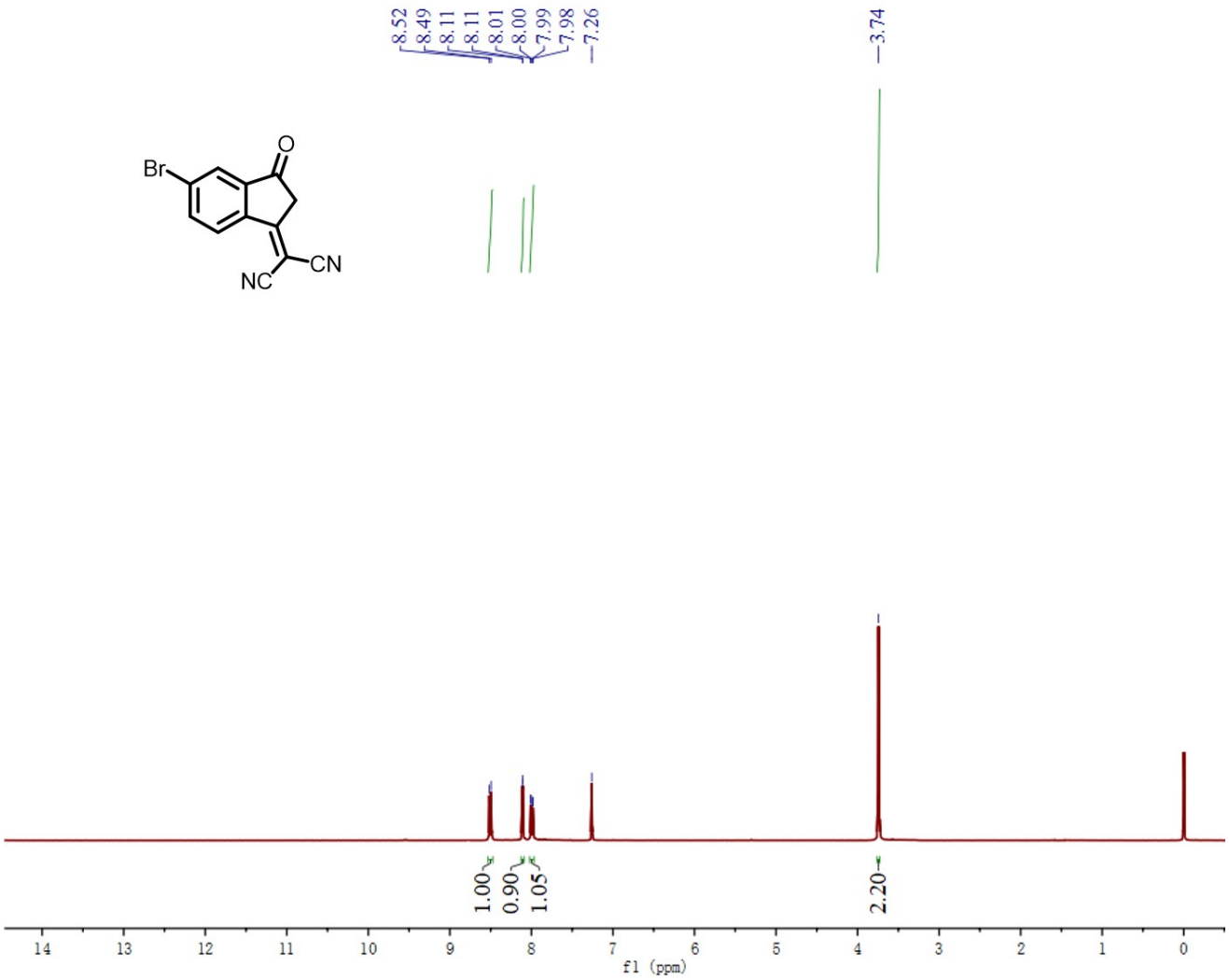

Figure S1. ^{1}H NMR spectrum of compound 2.

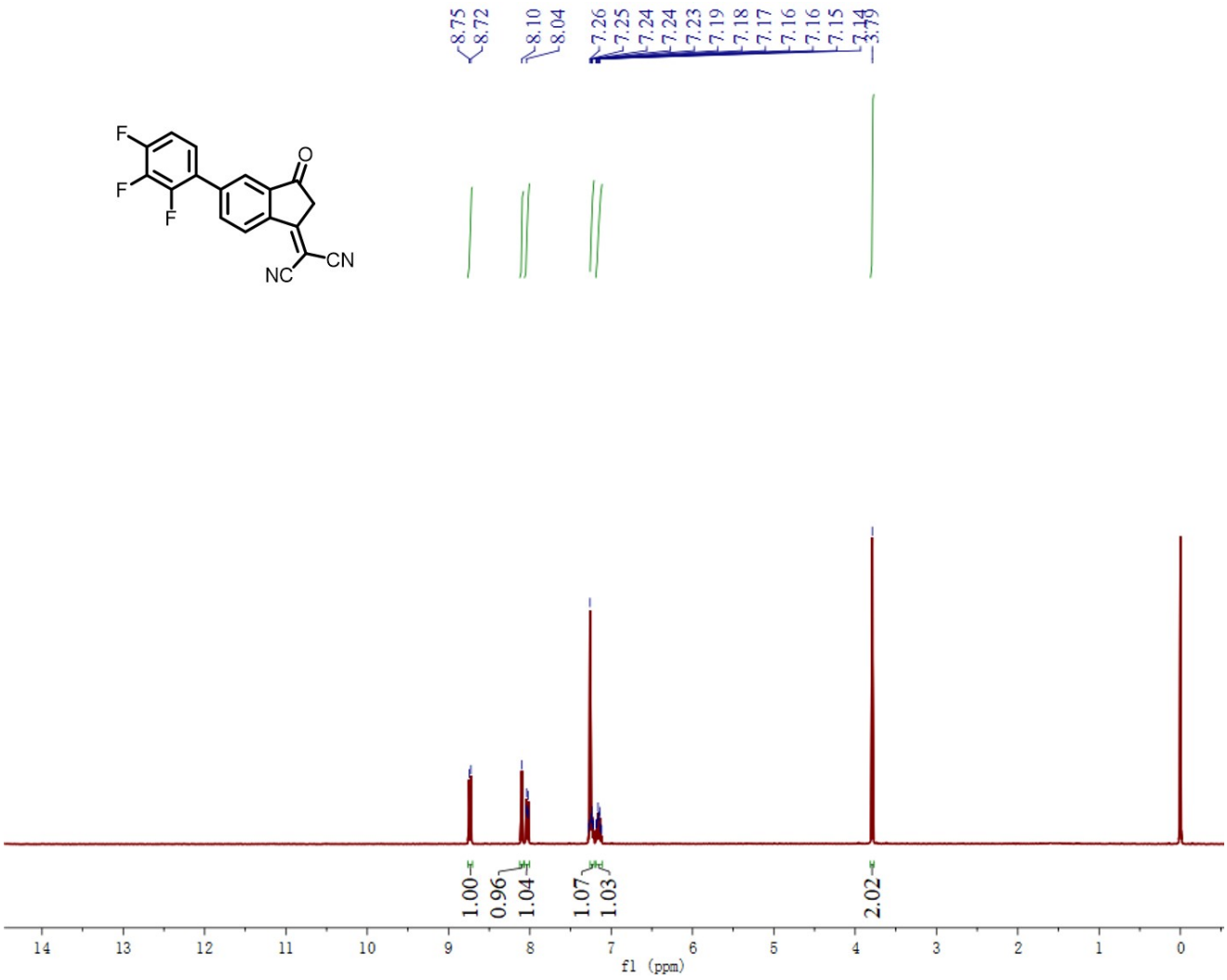

Figure S2. ^{1}H NMR spectrum of compound 4.

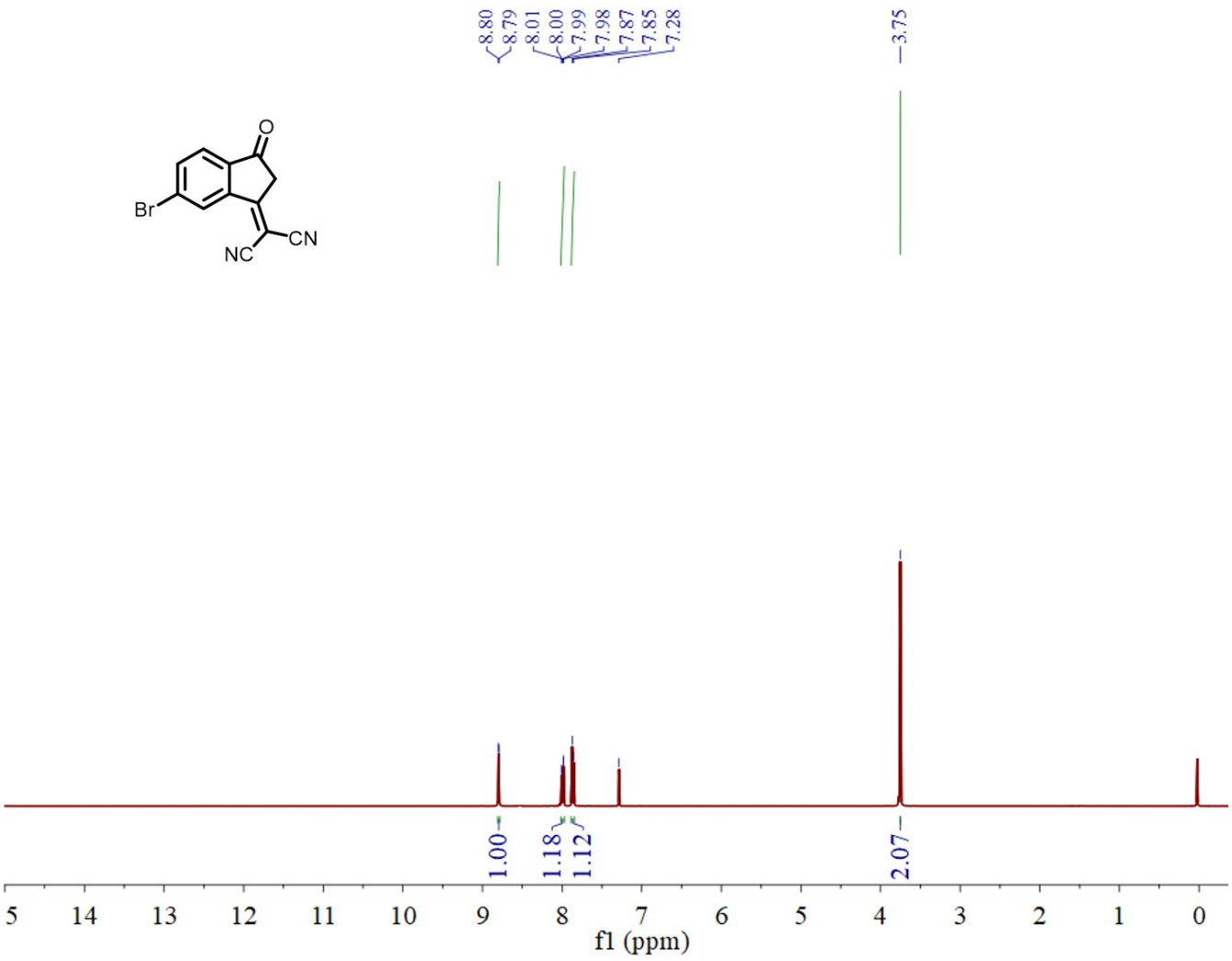

Figure S3. ^{1}H NMR spectrum of compound 3.

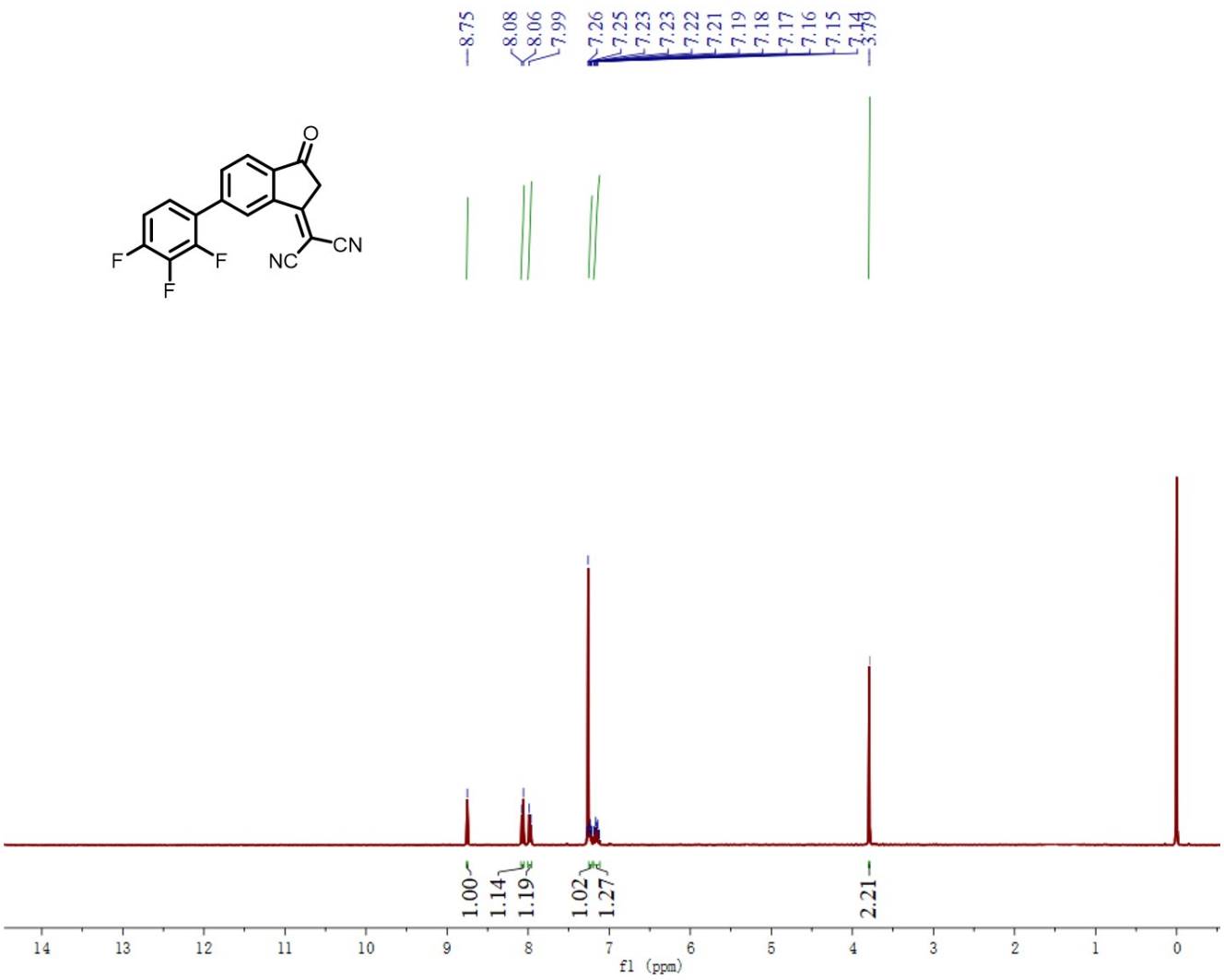

Figure S4. ^{1}H NMR spectrum of compound 5.

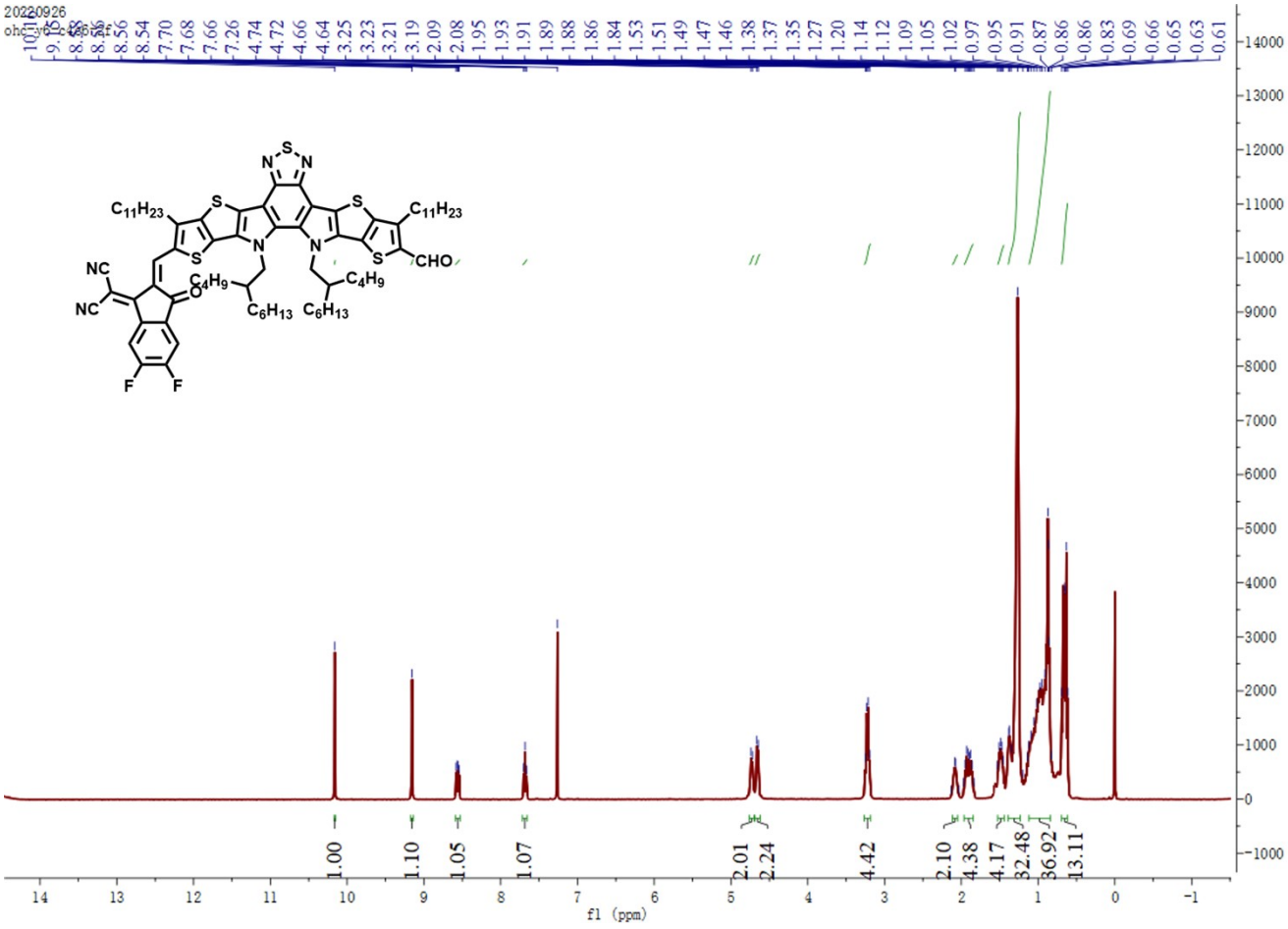

Figure S5. ^{1}H NMR spectrum of compound 6.

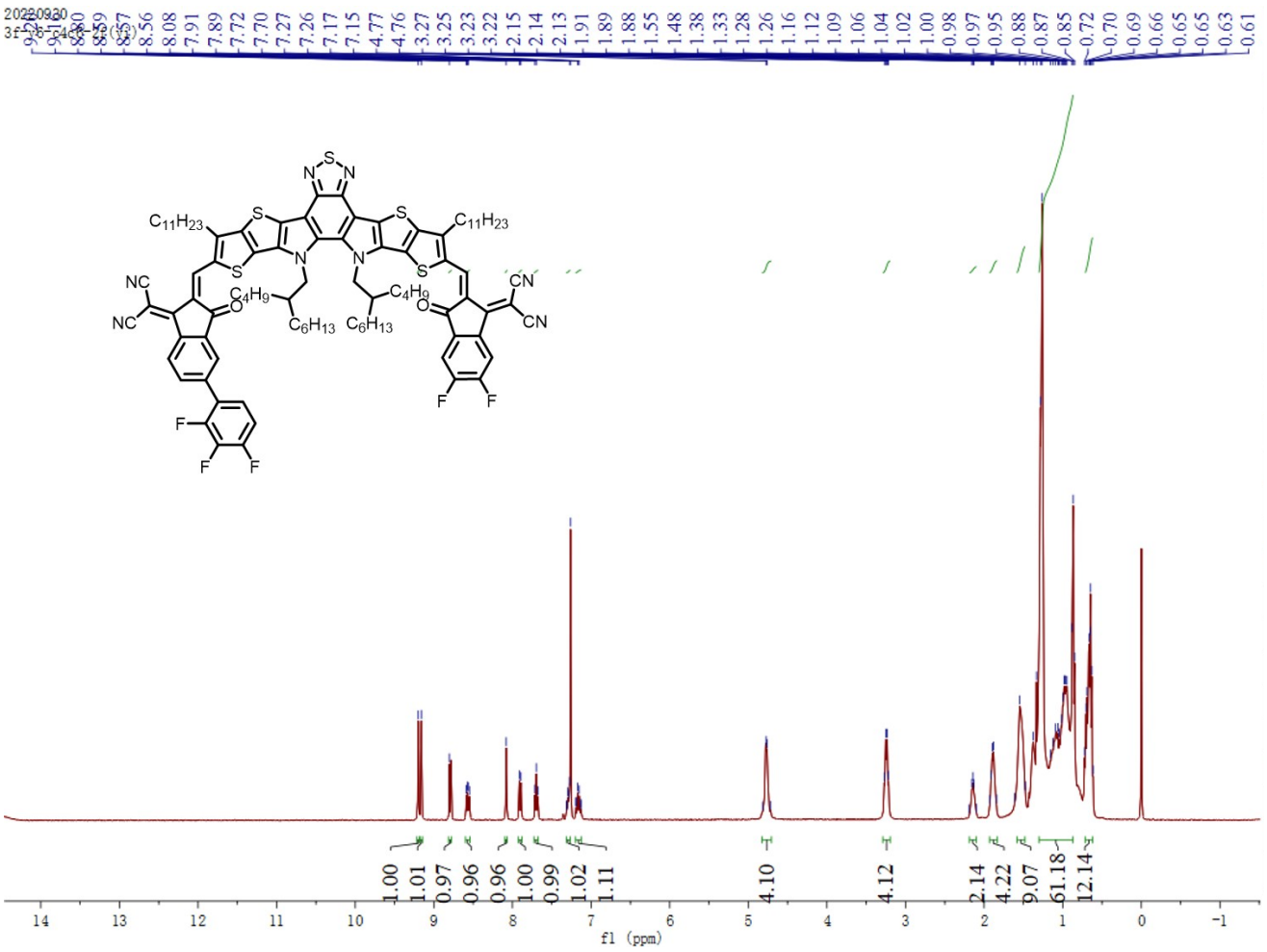

Figure S6. ^{1}H NMR spectrum of BTP-β-Ar3F.

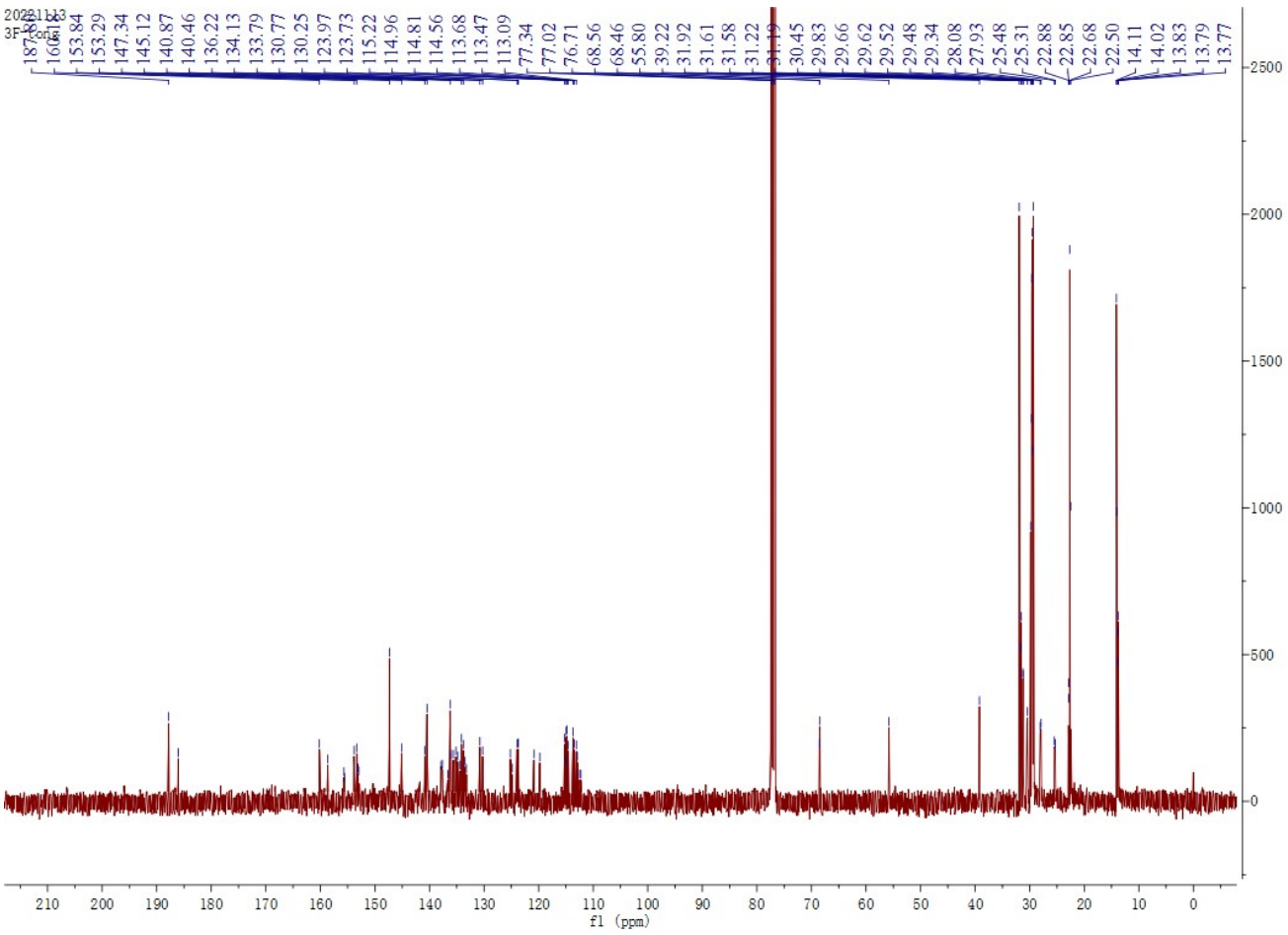

Figure S7. ^{13}C NMR spectrum of BTP-β-Ar3F.

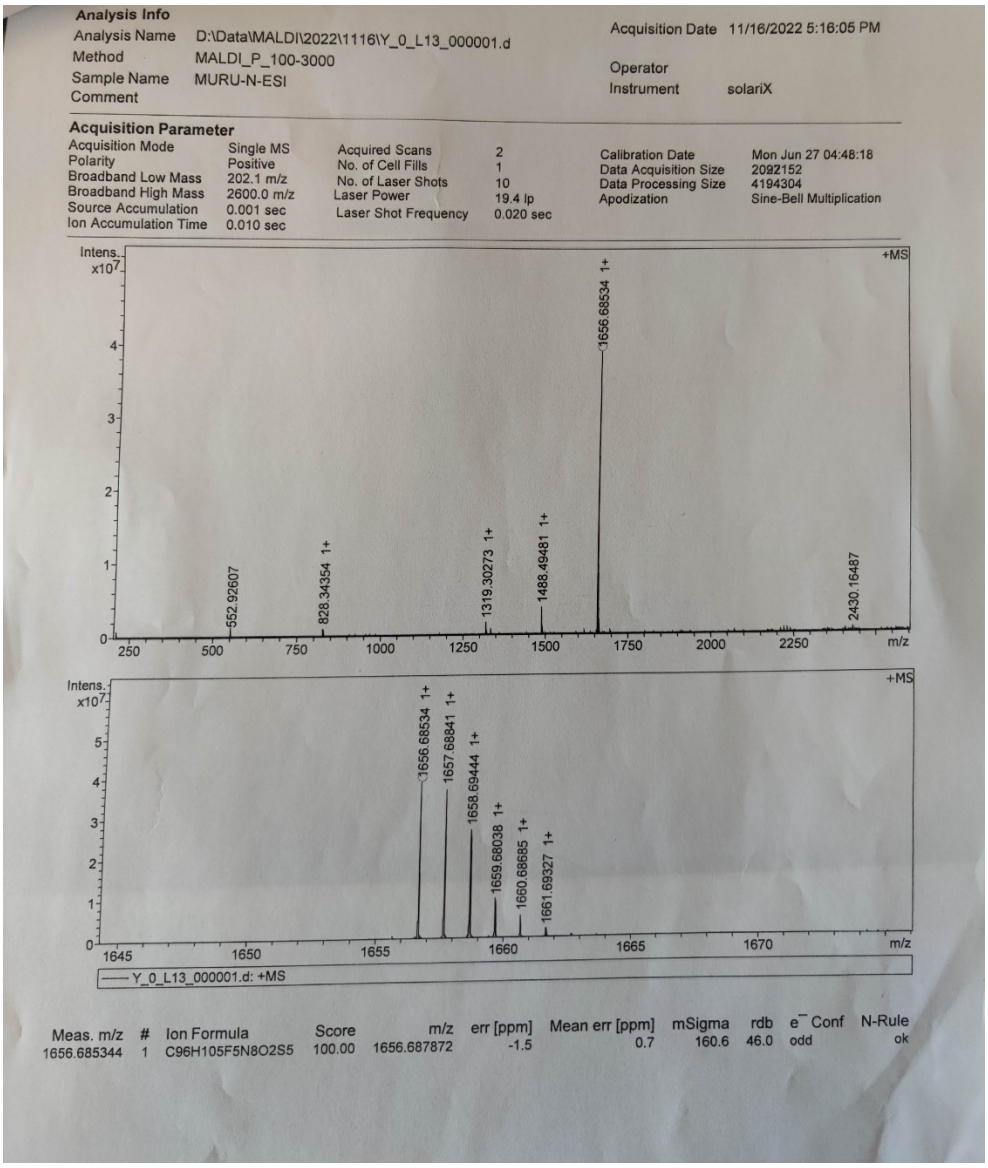

Figure S8. MALDI-TOF MS spectrum of BTP-β-Ar3F.

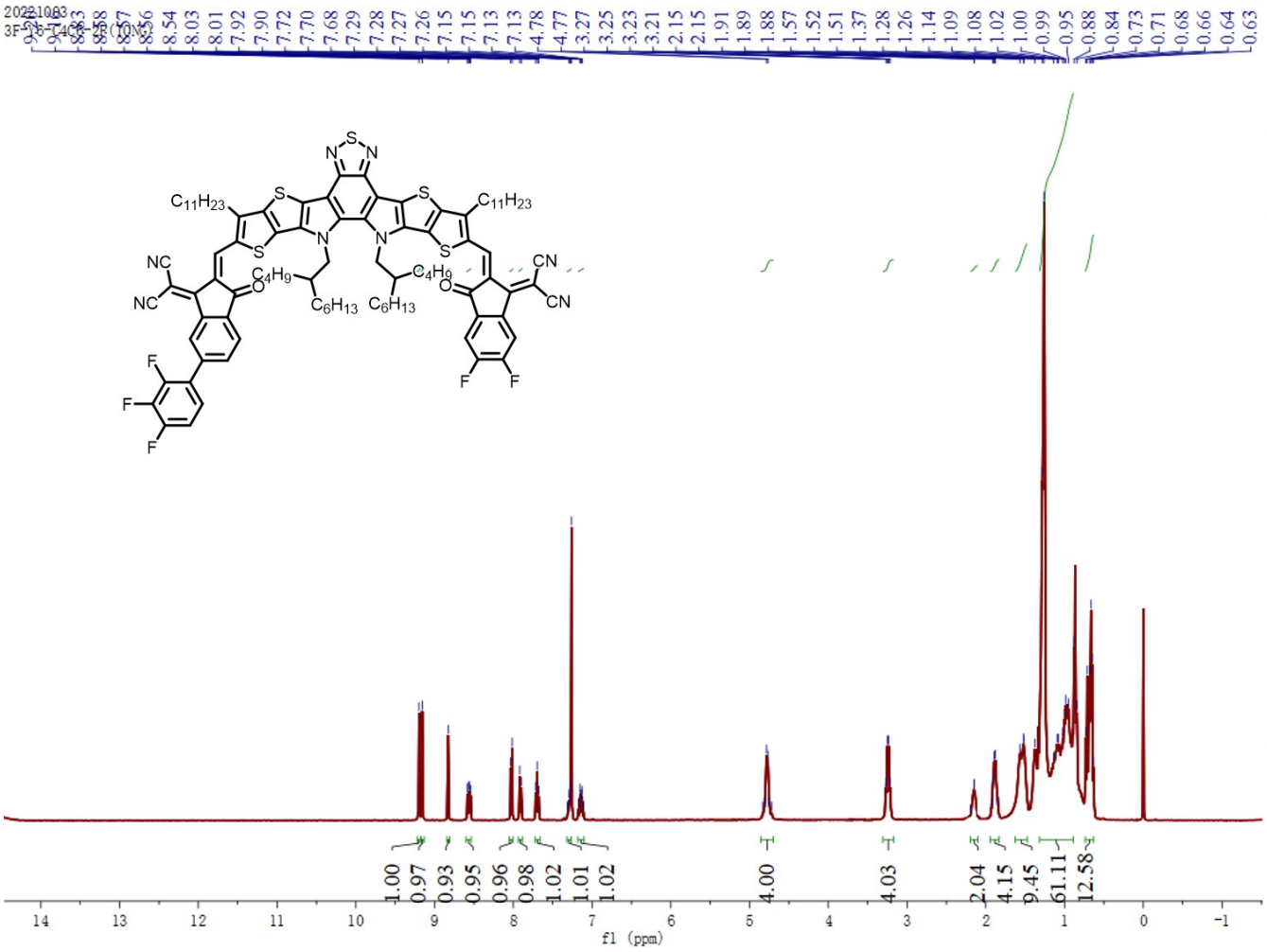

Figure S9. ^{1}H NMR spectrum of BTP-γ-Ar3F.

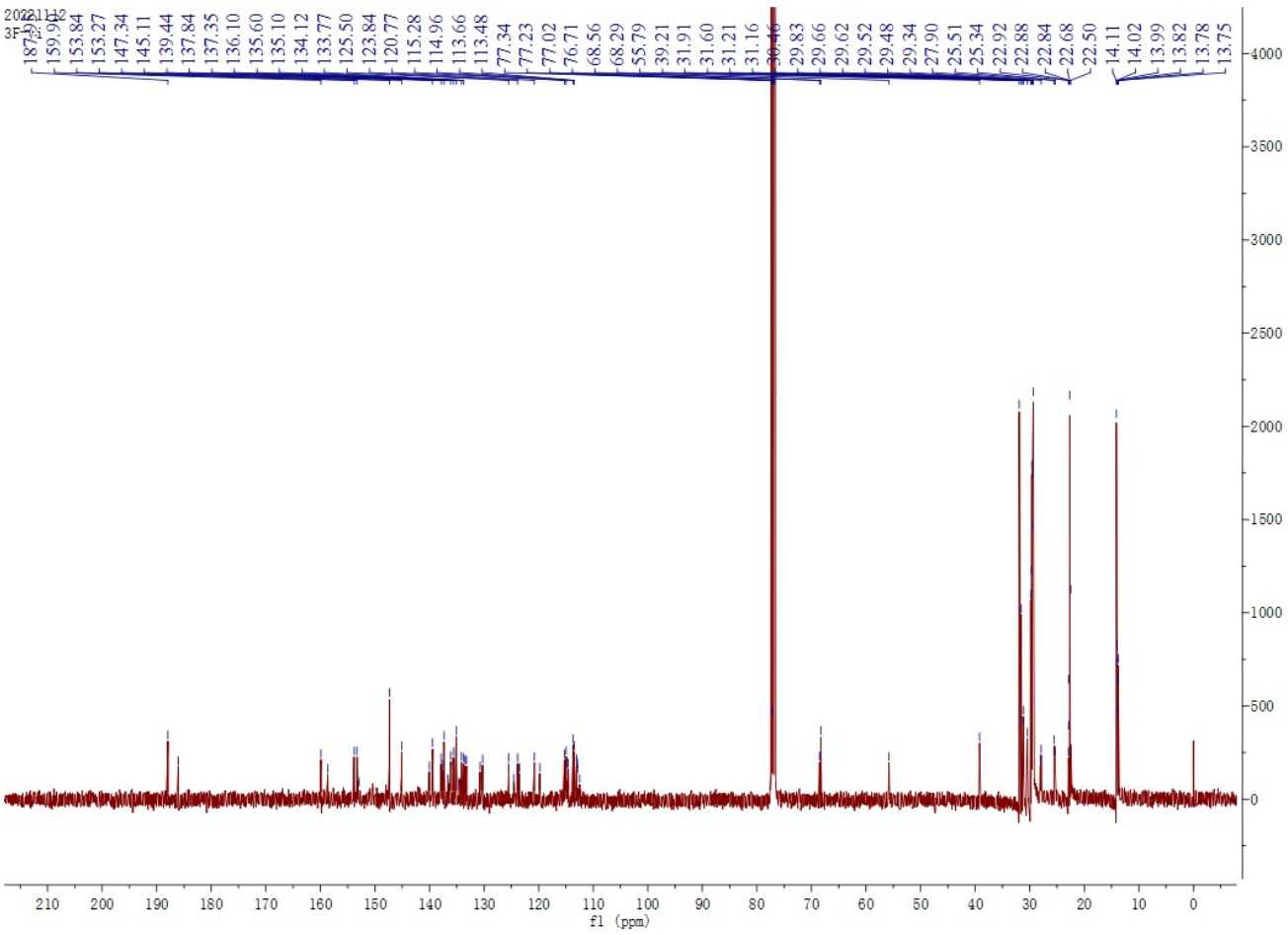

Figure S10. ^{13}C NMR spectrum of BTP-γ-Ar3F.

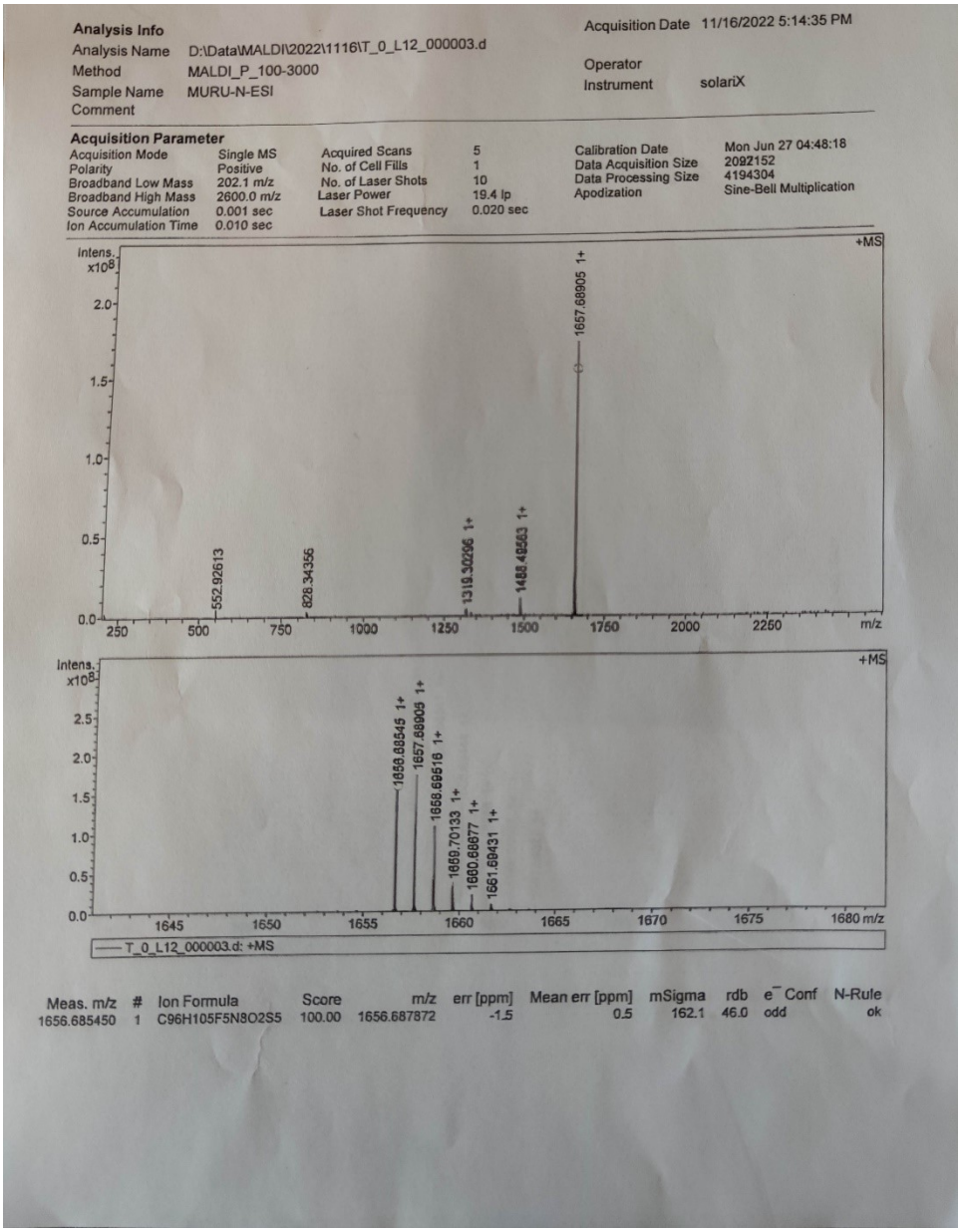

Figure S11. MALDI-TOF MS spectrum of BTP-γ-Ar3F.

2. Fabrication and characterization

OSCs fabrication and measurement:

The conventional device structure of ITO/PEDOT:PSS/active layer/PDINN/Ag was constructed. The indium tin oxide (ITO) substrates（purchased from Liaoning Preferred New Energy Technology Co., Ltd size of 15*15*1 mm, film thickness of 135 nm, sheet resistance 15 Ω sq-1） were prepared in ultrasonic baths in an order of containing detergent, water, deionized water, ethanol, then dried in oven at 80℃ for 10 min. The substrates were treated with ultraviolet ozone for 5 min and the PEDOT: PSS aqueous solution (Baytron P 4083 from H. C. Starck) was filtered through a 0.45 mm filter and then spin-coated on precleaned ITO-coated glass at 6000 rpm for 25 s. After annealing at 150℃ on hot plate in the air conditions for 15 min, the substrates were transferred into a N2 protected glove box. The optimal preparation process of the active layers is that the blend solutions of PM6:SMAs (BTP-β-Ar3F, BTP-γ-Ar3F) (1:1.2, w/w, and the total concentration was 16 mg/mL) in chloroform with the addition of a small amount of DIO (0.25%, v/v) were spin-coated on PEDOT:PSS films with 4500 RPM in a high purity nitrogen filled glove box. Then the active layers were annealed at 90 °C for 5 min. Detailed device fabrication conditions were summarized in Table. Then, ~10 nm PDINN as cathode interlayer was spin-coated onto the active layers in a concentration of 1 mg/ml in methanol solution. At last, about 100 nm Ag were vacuum thermally deposited on the top of the device through a shadow mask under 10^{-6} Pa vacuum conditions. The device area was exactly fixed at 4.0 mm^2. The current-voltage (J-V) curves of PSCs were measured in a high-purity nitrogen-filled glove box using a Keithley B2901A source meter. AM 1.5G irradiation at 100 mW cm-2 is provided by simulator (SS-F5-3A, Enlitech, AAA grade, 70× 70 mm^2 photobeam size) in glove box, which was calibrated by standard silicon solar cells. The external quantum efficiency (EQE) spectra of OSCs were measured in air conditions by a solar cell spectral response measurement system (QE-R3011, Enlitech).

***J-V* and EQE Measurement:** The current density-voltage (*J-V*) characteristic were measured by using the solar simulator (SS-F5-3A, Enlitech, Taiwan) along with AM 1.5G (100 mW/cm^2). The external quantum efficiency (EQE) was recorded with a QE-R measurement system (Enlitech, Taiwan). The effective area of all devices was confined as 0.06 cm^2.

Light-Intensity Dependence Measurements: Light-intensity dependence measurements were performed with PAIOS instrumentation (Fluxim) (steady-state and transient modes). Transient photo-voltage (TPV) measurements monitor the photovoltage decay upon a small optical perturbation during various constant light-intensity biases and at open-circuit bias conditions. Variable light-intensity biases lead to a range of measured V_{OC} values that were used for the analysis. During the measurements a small

optical perturbation (<3% of the V_{OC}, so that $\Delta V_{OC} << V_{OC}$) is applied. The subsequent voltage decay is then recorded to directly monitor bimolecular charge carrier recombination. The photovoltage decay kinetics of all devices follow a mono-exponential decay: $\delta V = A \exp(-t/\tau)$, where t is the time and τ is the charge carrier lifetime. The "charge extraction" (CE) technique was used to measure the charge carrier density n under open-circuit voltage condition. The device is illuminated and kept in open-circuit mode. After light turn-off, the voltage is switched to zero or taken to short-circuit condition to extract the charges. To obtain the number of extracted charges, the current is integrated. The carrier lifetimes follow a power law relationship with charge density: $\tau = \tau_0 n^{-\lambda}$. The bimolecular recombination constant k_{rec} were then inferred from the carrier lifetimes and densities according to $k_{rec} = 1/(\lambda+1)/n\tau^2$, where λ is the recombination order. Photo-CELIV measurements (ramp rate 100 V ms^{-1}, delay time: 0 s, offset voltage: 0 V, light pulse length: 100 μs) were also performed using PAIOS for different light intensities. The light intensity is given in the maximum power of the LED source (100% ≈ 100 mW cm^{-2}).

SCLC mobility measurement (SCLC): The structure of electron-only devices is ITO/ZnO/active layer/PDINN/Ag and the structure of hole-only devices is ITO/PEDOT:PSS/active layer/MoO3/Ag. In these device structures, the same fabrication conditions as OSCs are used to form the active layer films. The charge mobilities are generally described by the Mott-Gurney equation.[1]

$$J = \frac{9}{8}\mu\varepsilon_0\,\varepsilon_r V^2/L^3$$

where J is the current density, ε_0 is the permittivity of free space (8.85×10^{-14} F cm^{-1}), ε_r is the dielectric constant of used materials, μ is the charge mobility, V is the effective voltage. The effective voltage was obtained by subtracting the built-in voltage (V_{bi}) and the voltage drop (V_s) from the series resistance of the whole device except for the active layers from the applied voltage (V_{appl}), $V = V_{appl} - V_{bi} - V_s$. L is the active layer thickness. The ε_r parameter is assumed to be 3, which is a typical value for organic materials. In this case, the charge mobilities were estimated using the following equation:

$$\mu = \frac{8}{9}\varepsilon_0\,\varepsilon_r\left(\frac{\sqrt{J}}{V}\right)^2 L^3$$

^{1}H NMR and ^{13}C NMR: ^{1}H NMR,^{13}C NMR and ^{1}H-^{1}H NOESY NMR spectra were recorded on Bruker AVANCE 400 MHz NMR spectrometer with $CDCl_3$ as a solvent.

MALDI-TOF: MALDI-TOF mass spectrometry experiments were performed on an autoflex III instrument (Bruker Daltonics, Inc.).

TGA: TGA was measured on HTG-1 Thermogravimetric Analyzer (Beijing Hengjiu Experiment Equipment Co. Ltd.) with a heating rate of 10 °C min^{-1} under a nitrogen flow rate of 100 mL min^{-1}.

DSC: DSC measurements were performed on a Mettler Toledo DSC1 star system. The heating rate and cooling rate were both kept 10 ℃ min^{-1} under a nitrogen flow rate of 50 mL min^{-1}. The samples were loaded in aluminum pans directly with another empty aluminum pan as the reference. As for the blend samples, donor and acceptor materials were solved in chloroform (20 mg ml^{-1} for acceptor, gradient proportion of donor by mass concentration) and stirred overnight. Next the solvent was spin-coated onto cleaned glass substrates and dried under vacuum to form homogeneous films. The samples were then scraped off the substrates and loaded in aluminum pans.

UV-visible absorption: The UV-vis absorption spectra were measured by Hitachi U-2910 UV-vis spectrophotometer. In the case of solution absorbance measurement, the dilute solution of acceptors in chloroform (1×10^{-5} M) was prepared to be measured. Besides, the thin film samples were prepared by spin-coating (3000 rpm) acceptors' chloroform solutions (10 mg ml^{-1}) on quartz plates. The as-cast thin films all performed a thickness ranging from 50 nm to 80 nm, which were recorded on Bruker DEKTAK XT step profiler. Absorption spectra of acceptors at various annealing temperatures were measured *ex situ* to fit their T_g. After spin-coating, the thin films were annealed for 5 mins in air in various temperature (25 °C or 160 °C) depending on their nominal T_g.

Photoluminescence (PL): PL measurement was obtained through Fluorescence Spectrometer 5 from Edinburgh-instruments.

Cyclic voltammetry: Cyclic voltammetry was conducted on a Zahner IM6e electrochemical workstation using sample films coated on glassy carbon as the working electrode, Pt wire as the counter electrode, and Ag/AgCl as the reference electrode, in a 0.1 M tetrabutylammonium hexafluorophosphate (Bu4NPF6) acetonitrile solution and ferrocene/ferrocenium (Fc/Fc+) couple was used as an internal reference.

AFM: AFM measurements were performed by using Bruker Nano Inc. From America. All film samples were spin-cast on ITO substrates.

TEM: Transmission electron microscope (TEM) studies were conducted with a FEI Tecnai G2 F20 electron microscopy to investigate the phase distribution of the active layer，and with the scale bar is 200 nm

GIWAXS: The GIWAXS measurements were conducted at the Synchrotron Radiation Facility (SSRF), beamline BL14B1. Part of the GIWAXS data acquisition was also carried out at SSRF beamline BL16B1 and Beiiing Synchrotron Radiation Facility (BSRF) beamline 1W1A. Grazing incidence wide angle

scattering (GIWAXS) data were recorded at NCD-SWEET beamline (ALBA synchrotron in Cerdanyola del Vallès, Spain) with a monochromatic (λ = 960299 Å) X-ray beam of 80 × 30 μm2 [H × V], using a Si (111) channel cut monochromator. The scattered signal was recorded using a Rayonix LX255-HS area detector placed at 241.1 mm from the sample position. The reciprocal q-space and sample-to-detector distance were calculated using LaB_6 as calibrant. A near-critical angle of incidence of 0.13° was used to maximize the thin film signal and the collected 2D images were azimuthally integrated using PyFAI.[2]

3. Calculation methods

The Flory-Huggins interaction parameters (χ) of different blend films are evaluated via the T_m depression method of acceptors in homogeneous D: A mixtures with various D: A weight ratio.

The related calculation equation was developed by Nishi and Wang[3-7], as shown below:

$$\frac{1}{T_m}-\frac{1}{T_m^0}=-\frac{Rv_2}{v_1\Delta H_f}[\frac{ln\varphi_2}{m_2}+(\frac{1}{m_2}-\frac{1}{m_1})(1-\varphi_2)+\chi(1-\varphi_2)^2] \quad (1)$$

In Equation 1, subscripts 1 and 2 represent amorphous donor material and crystalline acceptor material, respectively; T_m and T_m^0 are the melting points of the D/A mixtures and the pure crystalline acceptors; ΔHf represents the heat of fusion of the crystalline acceptors; R is the ideal gas constant; v_1 and v_2 represent the molar volumes; m is the degree of polymerization; and φ is the volume fraction. In this work, subscripts 1 and 2 represent PM6 and SMAs, respectively. For the PM6/SMAs mixtures, since the degree of polymerization of PM6 is over large compared to SMAs, m_1 can be seen as ∞ and m_2 to be 1, so that Equation 1 can be simplified as:

$$\frac{1}{T_m}-\frac{1}{T_m^0}=-\frac{Rv_2}{v_1\Delta H_f}[ln\varphi_2+(1-\varphi_2)+\chi(1-\varphi_2)^2] \quad (2)$$

Moreover, χ can be of the following form if neglect the effects of entropy and φ_2,

$$\chi=\frac{\beta v_1}{RT_m} \quad (3)$$

where β represents the interaction energy density characteristic of the organic material pair. By substituting Equation 3 into Equation 2, Equation 4 is obtained as below, and the linear relationship between $-[1/T_m-1/T_m^0+Rv_2(\varphi_1+\ln\varphi_2)/(\varphi_1\Delta H_f)]/\varphi_1$ and φ_1/T_m represents the corresponding χ values.

$$-\frac{1}{\varphi_1}[\frac{1}{T_m}-\frac{1}{T_m^0}+\frac{Rv_2}{v_1\Delta H_f}(\varphi_1+ln\varphi_2)]=\frac{\beta v_2}{\Delta H_f}\cdot\frac{\varphi_1}{T_m} \quad (4)$$

Owen Method for calculating the surface energy. The Owen's method is often used to calculate the surface energy:

$$\gamma_s=\gamma_s^D+\gamma_s^P,\ \gamma_l=\gamma_l^D+\gamma_l^P \quad (5)$$

where γ_s is composed of the dispersion force γ_s^D and polarity force γ_s^P. γ_l is surface energy of the liquid and consists of a dispersion force γ_s^D and polarity force γ_s^P . We can know the surface energies γ_l^D and γ_l^P of the testing liquid and its contact angle on solid film. And according to the formula:

$$\gamma_l\,(1 + cos\theta) = 2(\gamma_s^D\gamma_l^D)^{1/2} + 2(\gamma_s^P\gamma_l^P)^{1/2} \qquad (6)$$

We need two known testing liquids to determine γ_s^D and γ_s^P .

$$\gamma_{l1}\,(1 + cos\theta) = 2(\gamma_s^D\gamma_{l1}^D)^{1/2} + 2(\gamma_s^P\gamma_{l1}^P)^{1/2} \qquad (7)$$

$$\gamma_{l2}\,(1 + cos\theta) = 2(\gamma_s^D\gamma_{l2}^D)^{1/2} + 2(\gamma_s^P\gamma_{l2}^P)^{1/2} \qquad (8)$$

Finally, γ_s can be determined by $\gamma_s = \gamma_s^D + \gamma_s^P$

Solubility parameter (δ) can be calculated from the surface tension,

$$\delta = K\sqrt{\gamma} \qquad (9)$$

where γ is the surface tension, K is the proportionality constant (K = 116 × 103 $m^{-1/2}$). And Flory–Huggins interaction parameter (χ_{ij}) can be written as a function of two solubility parameters,

$$\chi_{ij} = \frac{V_0}{RT}(\delta_i - \delta_j)^2 \qquad (10)$$

where χ_{ij} is the Flory–Huggins interaction parameter between the material i and j, V_0 is the geometric mean of the polymer segment molar volume, R is the gas constant, T is the absolute temperature, and δi and δj are the solubility parameter of material i and j, respectively. To simplify, we define the parameter $\kappa = \frac{\delta^2 V_0}{RT}$, then the Flory–Huggins interaction parameter can be written as the formula below,

$$\chi_{ij} = \kappa\,(\sqrt{\gamma_i} - \sqrt{\gamma_j})_2 \qquad (11)$$

where γ_i and γ_j are the surface tension of material i and j, respectively.

4. Supplementary figures

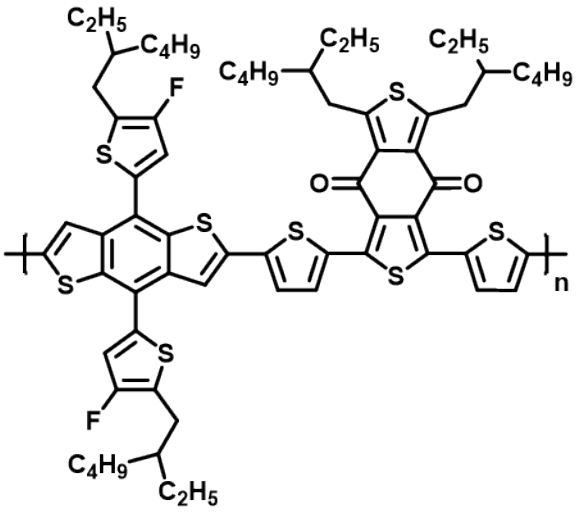

Figure S12. The molecular structures of PM6.

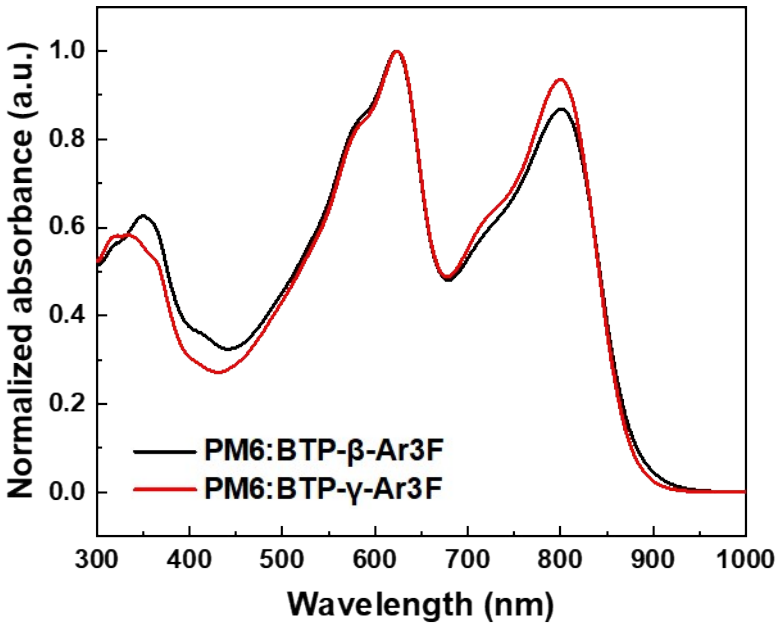

Figure S13. Normalized absorbance of PM6: BTP-β-Ar3F and PM6: BTP-γ-Ar3F in blend.

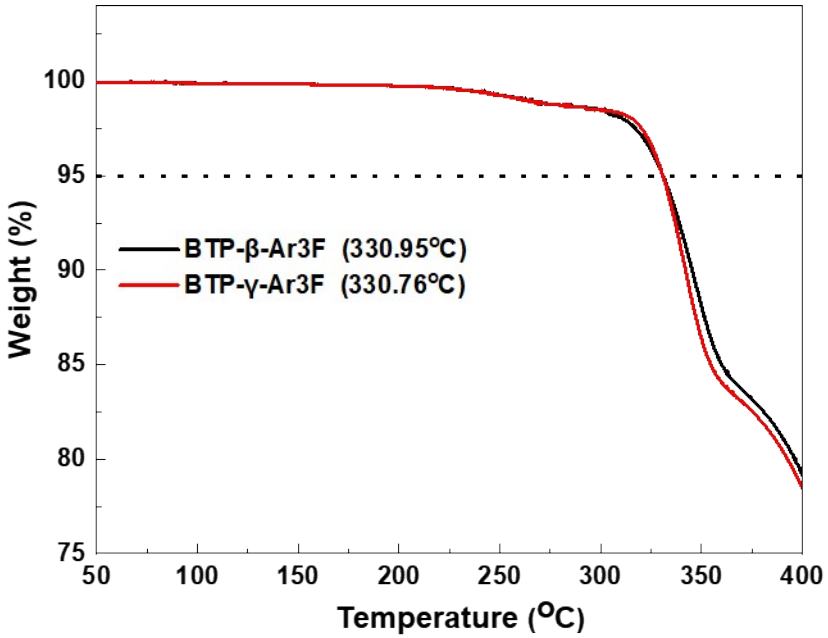

Figure S14. Thermal gravity analyzes (TGA) of BTP-β-Ar3F and BTP-γ-Ar3F with a heating rate of 10 °C/min under N2 atmosphere.

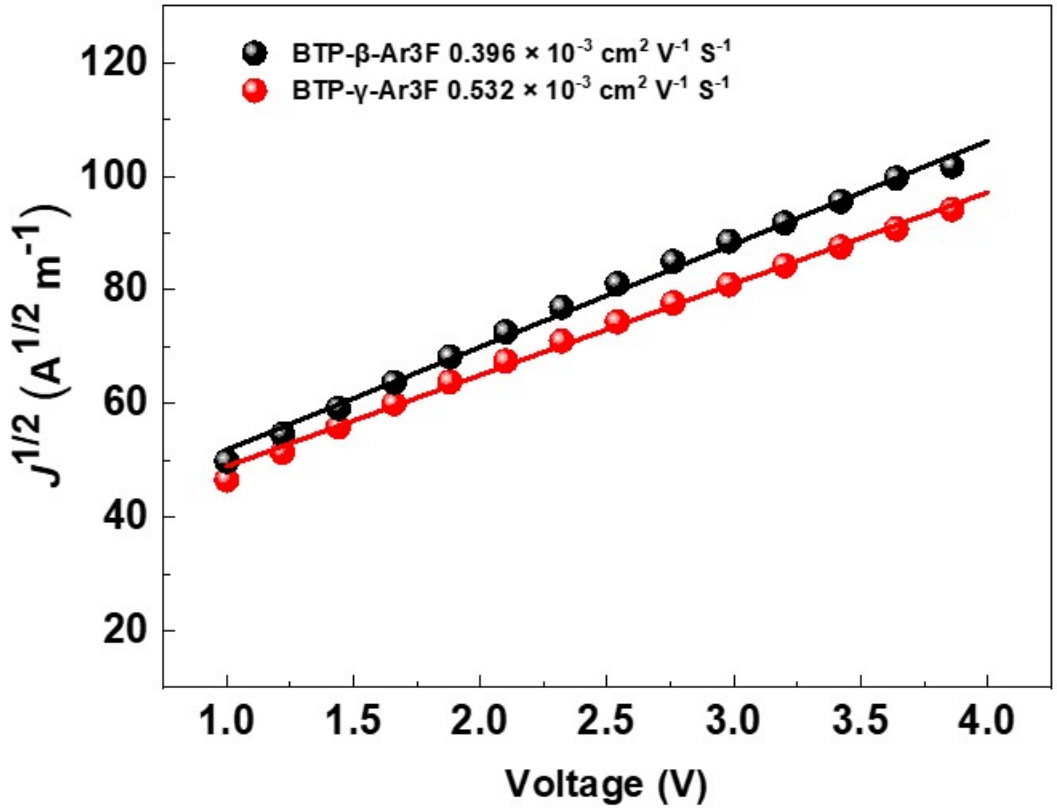

Figure S15. $J^{1/2}$-V curves of hole-only devices based on the BTP-β-Ar3F and BTP-γ-Ar3F film.

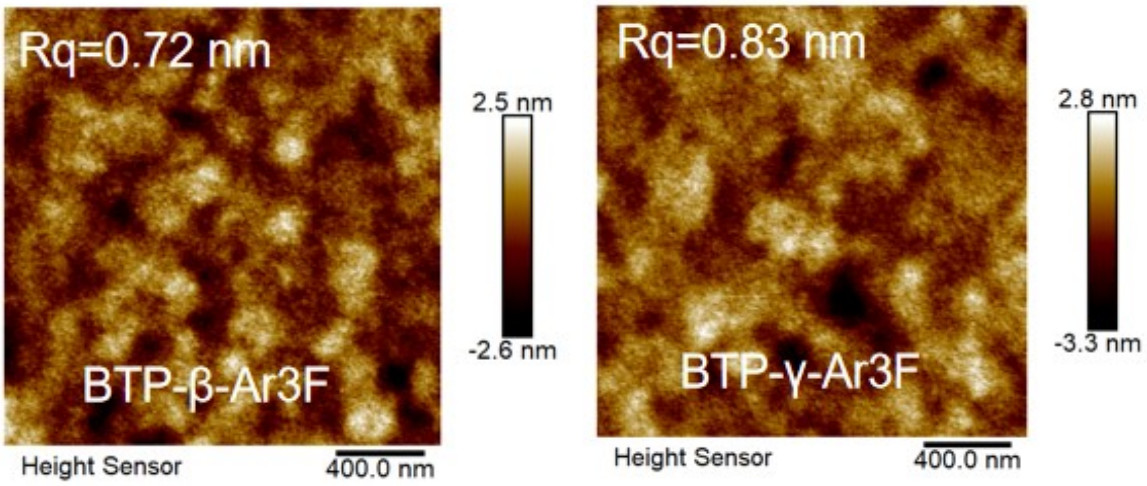

Figure S16. AFM phase images of (a) BTP-β-Ar3F, (b)BTP-γ-Ar3F films.

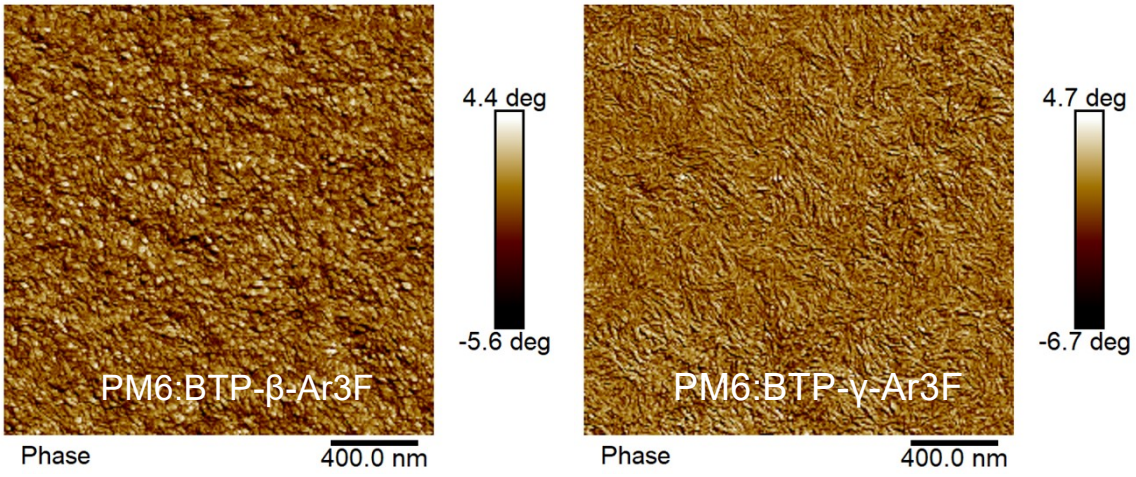

Figure S17. AFM height images of (a)PM6:BTP-β-Ar3F and (b)PM6:BTP-γ-Ar3F blend films.

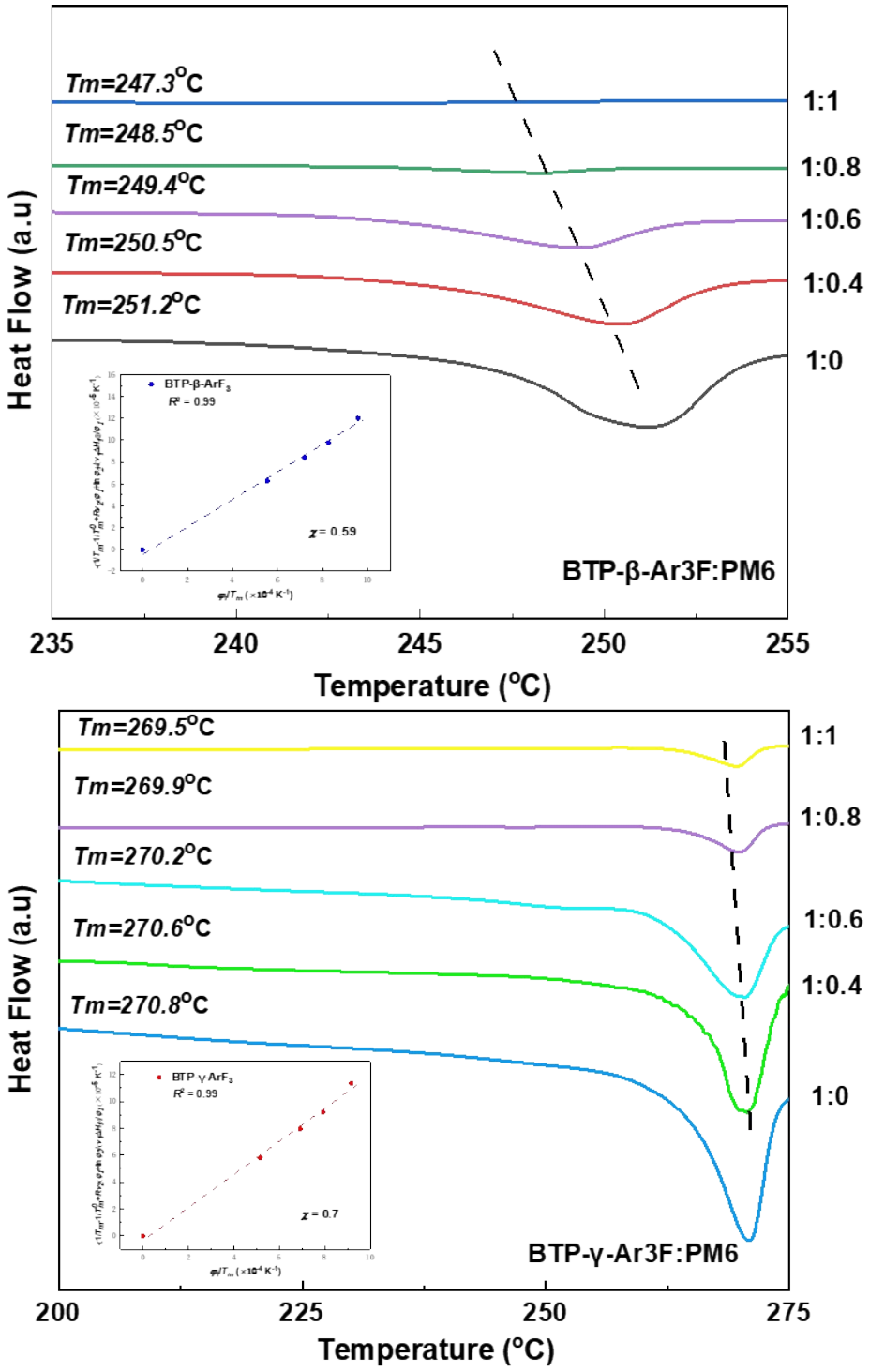

Figure S18. Estimates of the miscibility of (a) PM6:BTP-β-Ar3F, (b)PM6:BTP-γ-Ar3F from measurements of the melting point depression.

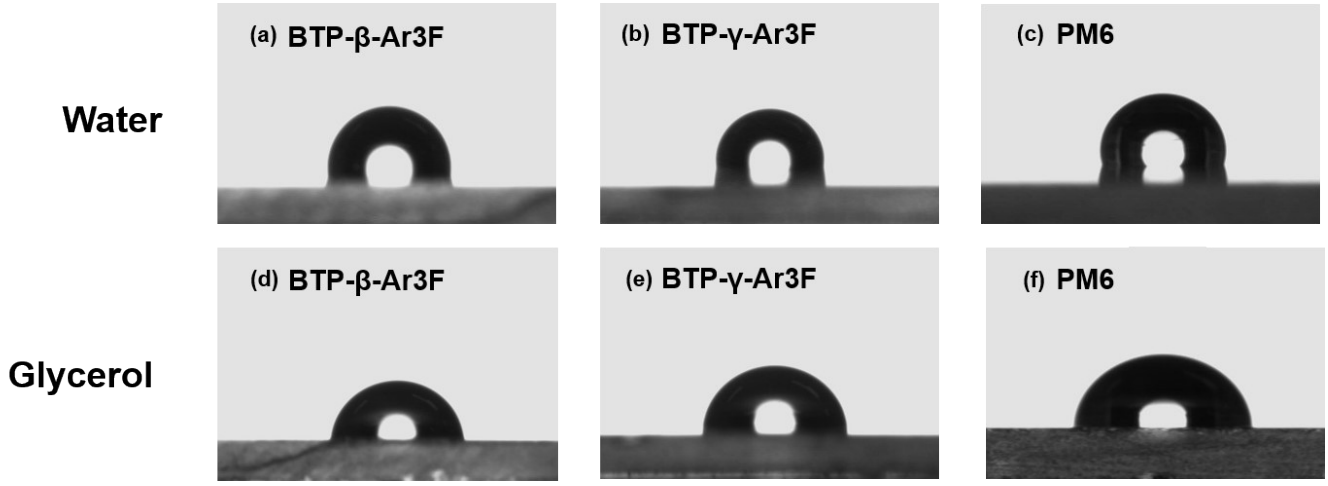

Figure S19. Photographs of water droplets on the top surfaces of (a) BTP-β-Ar3F (b) BTP-γ-Ar3F (c) PM6; and glycerol droplets on the top surfaces of (d) BTP-β-Ar3F (e) BTP-γ-Ar3F (f) PM6.

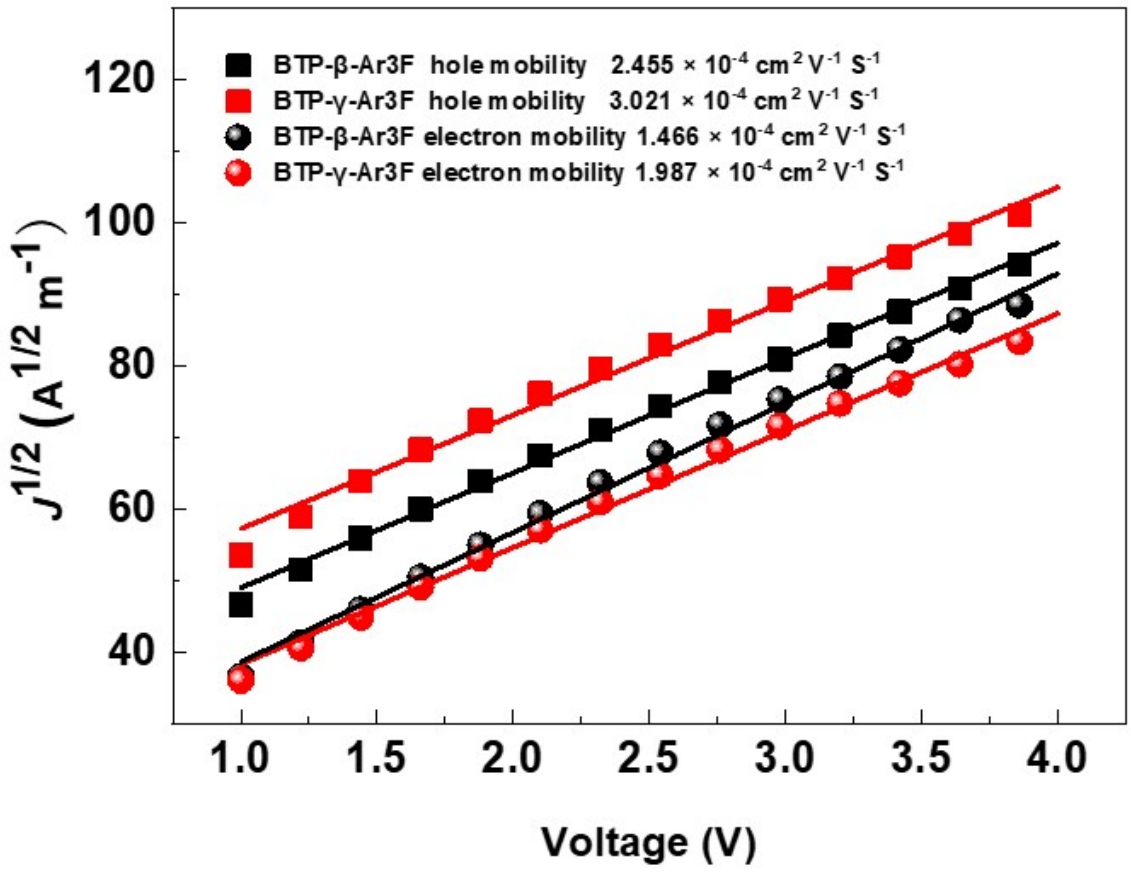

Figure S20. $J^{1/2}$-V curves of hole-only devices based on the(a) PM6:BTP-β-Ar3F and PM6:BTP-γ-Ar3F blend film,(b)BTP-β-Ar3F and BTP-γ-Ar3F film.

5. Supplementary figures

Table S1. DFT calculation results of BTP-β-Ar3F and BTP-γ-Ar3F, respectively.

Acceptor	HOMO (eV)	LUMO (eV)
BTP-β-Ar3F	-6.015	-4.012
BTP-γ-Ar3F	-6.004	-4.005

Table S2. The photovoltaic parameters of different treatment processes of PM6: BTP-β-Ar3F and PM6: BTP-γ-Ar3F.

Active layers	D:A (W: W)	TA [°C][b]	V_{oc} [V]	FF [%]	J_{sc} [mA cm-2]	PCE [%]	Addition [wt%]	RPM[c]	C [mg/ml]
PM6:BTP-β-Ar3F	1:0.8	None	0.915	67.32	24.02	14.80	None	4500	16
	1:1.2	None	0.91	68.85	24.63	15.43	0.15%DIO	4500	16
	1:1.2	None	0.913	70.36	24.85	15.96	0.25%DIO	4500	16
	1:1.2	80	0.901	72.50	25.01	16.34	0.25%DIO	4500	16
	1:1.2	90	0.900	73.32	24.83	16.38	0.25%DIO	5000	16
	1:1.2	90	0.898	73.96	24.93	16.56	0.25%DIO	4500	16
	1:1.2	90	0.892	72.03	25.04	16.09	0.25%DIO	4500	17
	1:1.2	90	0.892	71.82	25.15	16.11	0.25%DIO	4000	16
	1:1.2	100	0.885	70.26	25.34	15.76	0.25%DIO	4500	16
	1:1.2	None	0.894	68.46	24.98	15.29	0.35%DIO	4500	16
	1:1.6	None	0.907	63.33	23.52	13.51	None	4500	16
PM6:BTP-γ-Ar3F	1:0.8	None	0.917	57.22	22.58	11.85	None	4500	16
	1:1.2	None	0.918	68.68	23.51	14.82	None	4500	16
	1:1.2	None	0.911	70.67	24.82	15.98	0.15%DIO[a]	4500	16

	1:1.2	None	0.910	71.56	25.14	16.37	0.25%DIO	4500	16
	1:1.2	80	0.905	73.5	25.37	16.88	0.25%DIO	4500	16
	1:1.2	90	0.902	74.42	25.28	16.97	0.25%DIO	5000	16
	1:1.2	90	0.904	74.92	25.72	17.42	0.25%DIO	4500	16
	1:1.2	90	0.899	73.21	25.51	16.79	0.25%DIO	4000	16
	1:1.2	100	0.891	72.38	25.34	16.34	0.25%DIO	4500	16
	1:1.2	90	0.890	72.48	25.38	16.37	0.25%DIO	4500	17
	1:1.2	None	0.895	70.56	24.53	15.49	0.35%DIO	4500	16
	1:1.6	None	0.912	61.51	23.13	12.98	None	4500	16

[a]1,8-diiodooctane. [b]Thermal annealing treatment. [c]Spin-coating active layer rotation speed: round per minute. [d] .

Table S3. GIWAXS parameters of the pure films and the corresponding blend films in the OOP direction.

Device	Out-of-plane(010)		
	Location($Å^{-1}$)	d (Å)	CCL(Å)
PM6:BTP-γ-Ar3F	1.557	4.02	41.20
PM6:BTP-β-Ar3F	1.561	4.03	36.04
BTP-γ-Ar3F	1.535	4.09	7.39
BTP-β-Ar3F	1.505	4.17	5.67

Table S4. GIWAXS parameters of the pure films and the corresponding blend films in the IP direction.

Device	In-plane(100)		
	Location($Å^{-1}$)	d (Å)	CCL(Å)
PM6:BTP-γ-Ar3F	0.316	19.84	85.99
PM6:BTP-β-Ar3F	0.309	20.32	83.71
BTP-γ-Ar3F	0.361	17.40	31.58
BTP-β-Ar3F	0.331	18.93	6.33

Table S5. Surface energy for pure films calculated from water and ethylene glycol contact angle.

Film	Contact angle [°]		γ_s^d	γ_s^p	γ_s	χ
	Water	Ethylene glycol	[mN m^{-1}]	[mN m^{-1}]	[mN m^{-1}]	
PM6	102.5	89	18.56	1.39	19.95	---
BTP-β-Ar3F	93.4	78	25.14	2.30	27.44	0.60
BTP-γ-Ar3F	96.8	79.4	28.12	1.05	29.17	0.87

y_s^d is the dispersion component of surface free energy. γ_s^p is the polar component of surface free energy. γ_s is surface free energy. χ is the Flory-Huggins interaction parameter.

Table S6. The electron mobility (μ_e), hole mobility (μ_h) values of the PM6:BTP-β-Ar3F and PM6:BTP-γ-Ar3F blends-based OSCs by space-charge-limited current method(SCLC).

Active layers	μ_e [cm^2 Vs^{-1}]	μ_h [cm^2 Vs^{-1}]	μ_e/μ_h
BTP-β-Ar3F	0.396 ×10^{-3}	-	-
BTP-γ-Ar3F	0.532 × 10^{-3}	-	-
PM6:BTP-β-Ar3F	1.466 × 10^{-4}	2.455 × 10^{-4}	0.5971
PM6:BTP-γ-Ar3F	1.987 × 10^{-4}	3.021 × 10^{-4}	0.6577

6. References

1. W. Gao, F. Qi, Z. Peng, F. R. Lin, K. Jiang, C. Zhong, W. Kaminsky, Z. Guan, C. S. Lee, T. J. Marks, H. Ade and A. K. Jen, *Adv Mater*, 2022, **34**, e2202089.
2. G. Ashiotis, A. Deschildre, Z. Nawaz, J. P. Wright, D. Karkoulis, F. E. Picca and J. Kieffer, *Journal of Applied Crystallography*, 2015, **48**, 510-519.
3. T. Nishi and T. T. Wang, *Macromolecules*, 1975, **8**, 909-915.
4. Scott and L. Robert, *J. Chem. Phys.*, 1949, **17**, 279-284.
5. C. Zhang, A. Mumyatov, S. Langner, J. D. Perea, T. Kassar, J. Min, L. Ke, H. Chen, K. L. Gerasimov, D. V. Anokhin, D. A. Ivanov, T. Ameri, A. Osvet, D. K. Susarova, T. Unruh, N. Li, P. Troshin and C. J. Brabec, *Adv. Energy Mater.*, 2017, **7**, 1601204.
6. G. Wang, F. S. Melkonyan, A. Facchetti and T. J. Marks, *Angew. Chem. Int. Ed. Engl.*, 2019, **58**, 4129-4142.
7. M. Ghasemi, N. Balar, Z. Peng, H. Hu, Y. Qin, T. Kim, J. J. Rech, M. Bidwell, W. Mask, I. McCulloch, W. You,

A. Amassian, C. Risko, B. T. O'Connor and H. Ade, *Nat. Mater.*, 2021, **20**, 525-532.